Stretch-Induced Lncrna SNHG8 Inhibits Osteogenic Differentiation by Regulating EZH2 in Hpdlscs

Zijie Zhang
Shandong University School of Medicine: Shandong University Cheeloo College of Medicine
Qin He
Shandong University School of Medicine: Shandong University Cheeloo College of Medicine
Xiaolu Zhao
Shandong University School of Medicine: Shandong University Cheeloo College of Medicine
Xiaoyu Li
Shandong University School of Medicine: Shandong University Cheeloo College of Medicine
Fulan Wei (weifl@sdu.edu.cn)
Shandong University https://orcid.org/0000-0001-6827-8293

Research

Keywords: Long non-coding RNA, Mechanical force, Periodontal ligament stem cells, Osteogenic differentiation

Posted Date: March 30th, 2021

DOI: https://doi.org/10.21203/rs.3.rs-362066/v1

Abstract

Background: Periodontal ligament stem cells (PDLSCs) are important for the remodeling of the alveolar bone while tooth moving. However, the effect of long non-coding RNA (lncRNA) on osteogenic differentiation of PDLSCs under mechanical force remains unclear.

Methods: In this study, we compared stretched and non-stretched PDLSCs by high-throughput sequencing. The verification and selection of lncRNAs were achieved by quantitative reverse transcription polymerase chain reaction (qRT-PCR). PDLSCs osteogenic differentiation potentials were assessed by alkaline phosphatase (ALP) staining, Alizarin Red staining, qRT-PCR, and western blot. The application of mechanical force used Flexcell-FX-6000-Tension System *in vitro*, and constructing rats' tooth movement model *in vivo*. To verify the osteogenic regulation ability of small nucleolar RNA host gene 8 (SNHG8), PDLSCs were stretched or applied osteogenic induction after been infected by lentivirus. RNA fluorescence *in situ* hybridization, isolation of nuclear and cytoplasmic RNA, qRT-PCR and western blot were performed to locate SNHG8. Western blot and qRT-PCR to find the relationship between enhancer of zeste homolog 2 (EZH2) and SNHG8.

Results: Our results demonstrated that among lncRNAs altered screened by high-throughput sequencing, the expression level of SNHG8 steadily decreased after being stretched. Analysis of mRNA expression and protein levels revealed an upregulation of ALP and RUNX2, ALP and Alizarin Red staining showed more obvious alkaline phosphatase and more mineralized nodules in SNHG8 knockdown PDLSCs. *In vivo* experiments showed lower expression of the homologous gene of SNHG8 after tooth movement, and better ability of ectopic osteogenesis after knockdown SNHG8. The verification of SNHG8's nuclear location led us to infer that SNHG8 may interact with EZH2. The qRT-PCR and western blot results disclosed EZH2 expression reduced along with the knockdown of SNHG8. Furthermore, knockdown of EZH2 lead to PDLSCs' osteogenic differentiation ability increasing under osteogenic induction according to the mRNA level of ALP and RUNX2 accompanied by ALP and Alizarin Red staining results.

Conclusion: In general, our study confirmed that mechanically sensitive lncRNA SNHG8 can influence the osteogenic differentiation of PDLSCs through epigenetic pathways without directly encoding protein, which provides solid evidence for the regulation by non-coding genes.

Introduction

Human periodontal ligament stem cells (hPDLSCs) are stem cells derived from periodontal tissues, which have multiple ability to differentiate (1–3). PDLSCs are essential for the remodeling of the alveolar bone during orthodontic procedure (4, 5). According to classic pressure-tension theory (6), force-induced bone remodeling is caused by cell differentiation in the presence of osteogenic-related chemical messengers, cytokines such as hydrogen sulfide, transcription factors such as RUNX2, and the Wnt/β-catenin pathway (7–9).

Mechanical force is a common stimulation in physiological and pathological activities. With the continuous in-depth research such as cell behavior and tumor formation, scholars have discovered that mechanical force not only can guide the differentiation and proliferation of cells in embryonic development, but also participates in the development of force-related organs and tissues. Furthermore, it also plays an important role in determining the fate of stem cells (10). Since orthodontics provide a cellular environment closely related to mechanical forces, our previous studies have focused on mechanical force-related genes and their ability to affect osteogenic differentiation. We found the express pattern and the function of coding and non-coding genes induced by mechanical force and their downstream pathway (11, 12). Then a series of microRNAs (miRNAs) analysis experiments proved miR-21 as a key miRNA related to mechanical force induced osteogenic differentiation (13). We also confirmed that long non-coding RNAs (lncRNAs) and mRNAs can competitively interact with the same miRNA (14). The close relationship between miRNAs and lncRNAs is one of the bases to deduce the cellular physiology function of lncRNAs. However, it remains to be determined if there are mechanical force-sensitive lncRNAs, and whether these lncRNAs can regulate the osteogenic differentiation of hPDLSCs under mechanical force.

LncRNAs are a type of non-coding RNA with a length of more than 200 nucleotides. They were previously regarded as genetic “noise” because they do not encode proteins. In recent decades, the development of high-throughput sequencing has allowed researchers to further study this field(15, 16). LncRNAs can bind to and target chromatin regulators, act as RNA enhancers (17), interact with miRNAs (18, 19), and mediate related signaling pathways, thereby regulating physiological and pathological processes (20, 21) at the transcription and post-transcription levels (22, 23). The mechanically sensitive lncRNA small nucleolar RNA host gene 8 (SNHG8), which was screened through high-throughput sequencing, was showed to interact with enhancer of zeste homolog 2 (EZH2) based on the RNA immunoprecipitation assay (24). SNHG8 is a member of the SNHG family of genes, which is closely related to the prognosis and progression of a variety of cancers, and plays a key role in regulating tumor progression and cell proliferation (25–27). EZH2 is one of the core subunits of polycomb repressive complex 2 (PRC2), and the correlation between EZH2 and mesenchymal stem cell (MSC) osteogenic differentiation has been confirmed (28–30).

In this study, the high-throughput sequencing results were screened for lncRNAs with high Kyoto Encyclopedia of Genes and Genomes (KEGG) and Gene Ontology (GO) scores, which found considerable lncRNAs showed difference in expression level after being stretched. We selected several lncRNAs and verified their changes in expression using quantitative reverse transcription polymerase chain reaction (qRT-PCR). Then we knocked down SNHG8 to determine whether lncRNA silencing could alter osteogenic differentiation under stretching or osteogenic induction in a series of experiments. The *in vivo* experiments achieved consistent results. We also confirmed the interaction between SNHG8 and EZH2, and verified the close relationship between the expression level of EZH2 and the osteogenic differentiation of hPDLSCs.

Materials And Methods

Ethics statement

All protocols for treating periodontal ligament tissues were performed in accordance with relevant guidelines and regulations. This study was approved by the Research Ethics Committee of Shandong University (No. G201401601). Informed consent was obtained from the donors and their parents before treatment. The research methods of animal experiments in this study are consistent with routine, and the experimental design was confirmed with the principles of animal protection. This study was approved by the Committee on the Ethics of Animal Experiments of Shandong University (No. 20190503).

Cell isolation, culture, and identification

In this study, 46 premolars without caries or periodontitis from 33 donors aged 12-20 years were obtain for orthodontic purposes. The isolation and culture of PDLSCs were performed as previously reported (31, 32). The premolars were extracted at the Department of Oral Maxillofacial Surgery, School of Stomatology, Shandong University (Jinan, China). We used flow cytometry (Becton Dickinson, Franklin Lakes, NJ, USA) to detect the cell surface markers including cluster of differentiation 31 (CD31), CD45, CD146, and Stro-1 (33).

Application of mechanical force *in vitro*

Mechanical force was applied using the Flexcell-FX-6000-Tension System (Flexcell International Corporation, Burlington, NC USA). PDLSCs were seeded onto flexcell Amino silicone-bottomed plates 6 well cell culture plates coated with collagen I solution (Collagen I, rat Tail, Corning, NY, USA) at a density of 2.0×10^6 cells per well. After the density reached ~80% confluence, the cells were serum deprived (2% serum) for 24 h before stretching. We imposed 10% stretch at 0.5 Hz. The control group was cultured in same silicone bottomed plates and the same culture environment without stretching.

High-throughput sequencing

Total RNA was extracted from the non-stretched and stretched groups of cells using RNAiso TM Plus (Takara, Shiga, Japan) according to the manufacturer's protocols. Strand-specific cDNA libraries were constructed following a previously described protocol (34) and were sequenced on the Illumina HiSeq 2000/2500 sequencer (LC Biotech, Guangzhou, China). Sequencing was done according to the HiSeq 2000 User Guide with paired-end program.

RNA extraction and quantitative reverse transcription polymerase chain reaction (qRT-PCR)

Total RNA was isolated from PDLSCs using RNAiso TM Plus (Takara) according to the manufacturer's protocol. The extracted total RNA was reverse-transcribed using the Prime Script RT Reagent Kit with gDNA Eraser (Takara). Relative RNA level was detected using the LightCycler-480 system (Roche Diagnostics GmbH, Mannheim, Germany) and TB Green Premix Ex Taq II (Takara). GAPDH and U6 were

used as internal controls to quantify and normalize the results. The PCR reaction conditions were as follows: 95 ℃ for 30 s, then 55 cycles of 95 ℃ for 10s, 60 ℃ for 30 s. The 2-ΔΔCT value was used for comparative quantitation. The sequences of primers are shown in Table 1. All PCR processes were performed in triplicate.

Cell transfection

SNHG8 and EZH2 knockdown was conducted via lentiviral transfection (Genechem, Shanghai, China). Regarding SNHG8, two lentiviral constructs designated sh-SNHG8-1# and sh-SNHG8-2# were generated based on different regions of the human SNHG8 sequence (NCBI Gene ID: 100093630). For EZH2 knockdown, we constructed sh-EZH2 based on previous researches (35). The negative control containing a nonspecific RNA oligonucleotide was constructed as previously described (36, 37). Cells were observed under a fluorescence microscope and an inverted phase contrast microscope (TH4-200; Olympus, Tokyo, Japan).

Induction of osteogenic and adipogenic differentiation.

We cultured hPDLSCs in osteogenic-inducing medium containing 100 μM ascorbic acid (Sigma-Aldrich, St. Louis, MO, USA), 2 mM β-glycerophosphate (Sigma), 10 nM dexamethasone and 0.1 mg/mL penicillin-streptomycin (Biosharp, Hefei, China). Alkaline phosphatase (ALP) staining (Solarbio, Beijing, China) and 1% Alizarin Red S (Sigma) staining were used to evaluate the effect of osteogenic induction. For adipogenic-induction, we cultured hPDLSCs in medium containing of 1 μM dexamethasone, 200 μM indomethacin (Sigma), 10 μM insulin (Sigma), 0.5 mm isobutyl methylxanthine (Sigma), and 0.1 mg/mL Penicillin-Streptomycin Solution (Biosharp) for two weeks to achieve the adipogenic differentiation. Oil Red O staining (Solarbio) was used to identify lipid-laden fat cells.

Western blot analysis

PDLSCs were collected and lysed in RIPA reagent (Solarbio) containing 1% PMSF. After heating, the protein samples were separated in a 10% sodium dodecyl sulfate polyacrylamide gel electrophoresis gel and transferred to a 0.2 μm polyvinylidene fluoride membrane (Millipore, Burlington, MA, USA). After blocking in 5% skimmed milk, membranes were incubated overnight at 4 ℃ with the following primary antibodies: rabbit anti-RUNX2 (1:1000, Lot # 8486S; Cell Signaling Technology, MA, USA), rabbit anti-ALP (1:1000, 11187-1-AP; Proteintech, Rosemont, IL, USA), rabbit anti-EZH2 (1:500, Lot # 2477979; Millipore), rabbit anti-embryonic ectoderm development (EED) (1:500, 16818-1-AP; Proteintech), rabbit anti-suppressor of zeste 12 (SUZ12) (1:500, 20366-1-AP; Proteintech) and rabbit anti-GAPDH (1:2000, 10494-1-AP, Proteintech, USA). After washing in Tris-buffered saline solution (TBS-T, Solarbio) with Tween-20, the membranes were incubated at room temperature for 1 h with peroxidase-conjugated anti-rabbit IgG (SA00001-2; Proteintech). ECL chromogenic substrate (Millipore) was used to detect the immunoreactive bands, and ImageJ software (National Institutes of Health, Bethesda, USA) was used to quantify the densitometry using GAPDH as the control.

Construction of tooth movement model *in vivo*

Twenty five 6-week-old male wistar rats (Charles River, Beijing, China) were used for the construction of tooth movement model *in vivo*. All rats were fostered 12/12 h day/night cycle to simulate common environment, and were adaptively fed for 3 days before experiment. The maxillary left first molar and the upper incisors were ligatured by 0.25 mm stainless steel with a nickel-titanium closed-coil spring (TOMY, Japan) in between. The nickel-titanium spring provide a force of approximate 20 g. In order to fix the structure, we drilled grooves at the left upper incisor tooth cervix, and fixed with light-curing resin. To avoid the individual differences of rats, each rat was performed tooth movement operation on dentition of the left maxillary, and the right side was not operated as a self-control. After retained the structure for 3 days, 7 days, 14 days, and 21 days, the periodontal tissues (include alveolar bone and periodontal ligament) were isolated for qRT-PCR.

Ectopic osteogenesis *in vivo*

The osteogenic differentiation potential of PDLSCs with different SNHG8 expression levels were tested by *in vivo* ectopic bone formation analysis. Briefly, untransfected hPDLSCs (Control group), hPDLSCs transfected with empty plasmids (sh-NC group), and hPDLSCs transfected with effective lentivirus (sh-SNHG8 group) were transferred subcutaneously to 5-week-old nude mice (Charles River) with osteo-inductive calcium phosphate bioceramic material (TH/P 1020, Sichuan University, China). After 10 weeks of fostering, the nude mice were executed and the ectopic bone formation under the skin was harvested. After decalcification treatment, HE staining (Solarbio), Masson's trichrome staining (LEAGENE, Beijing, China) and SafraninO-staining (Solarbio) were performed according to the manufacturer's instructions.

Isolation of nuclear and cytoplasmic RNA

The nucleus and cytoplasm of PDLSCs were separated using the Ambion® PARIS™ Kit (Life Technologies, Frederick, MD, USA) according to the manufacturer's instructions. We lysed approximately 5.0×10^6 cells in ice-cold cell fractionation buffer, and separated the cytoplasmic fraction from the nuclear fraction by low-speed centrifugation. Then we lysed the nuclear fraction in cell disruption buffer. Two kinds of fraction were mixed with lysis/binding solution separately, washed with washing solution, and eluted with preheated elution solution. For qRT-PCR, GAPDH was used as the control for the nuclear fractions and U6 was the control for the cytoplasmic fractions.

RNA fluorescence *in situ* hybridization

The fluorescence *in situ* hybridization (FISH) assay was performed using a Fluorescence In Situ Hybridization Kit (Ribobio, Guangzhou, China) according to the manufacturer's instructions. After fixed in 4% paraformaldehyde, PDLSCs were washed with phosphate-buffered saline containing 0.5% Trition X-100 to increase cell permeability. We observed PDLSCs with an inverted phase contrast microscope (DMi8; Leica, Germany) after incubating PDLSCs overnight at 37 °C with hybridization solution

containing the SNHG8, U6 and 18S probes. The excitation wavelengths were 405 nm for DAPI and 488 nm for the probes.

Statistical analysis.

All statistical calculations were performed using SPSS19.0 (SPSS Inc., Chicago, IL, USA). All data are normally distributed and presented as the mean±standard deviation of three to five independent samples. Differences between the results obtained from various experimental groups were analyzed by the Student's *t*-test or one-way analysis of variance. $P < 0.05$ was considered statistically significant.

Results

Cell culture and identification of biological characteristics

The cultured cells had the typical spindle-shaped structure of hPDLSCs (Fig. 1A). According to the negative results for CD31 and CD45, positive results for CD146 and Stro-1 by flow cytometry, we confirmed that hPDLSCs were isolated (Fig. 1B). To verify the osteogenic and adipogenic differentiation of PDLSCs, we induced osteogenic and adipogenic differentiation induction *in vitro*. Then we performed ALP staining and Alizarin Red S staining to identify the osteogenic differentiation level, and Oil Red O staining to evaluate the adipogenic differentiation level. There were more calcium nodules in the osteogenic induction group were more than in the non-induction group (Fig. 1C, D). And the Oil Red O staining shown that the adipogenic induction group had successfully induced differentiation of lipid-laden fat cells compared with the non-induction group (Fig. 1E).

Identification of mechanical force-sensitive lncRNA

In order to select lncRNAs that showed different expression levels, we applied tension force to the hPDLSCs (Fig. 2A) and subjectived non-stretched and stretched groups of hPDLSCs to high-throughput sequencing. The detailed sequencing results have been published (14). The results showed that 14 704 lncRNAs had different expression levels after being stretched, of which 7 526 were known lncRNAs and 7 178 were unknown lncRNAs. To narrow the range, lncRNAs were selected with more than three times the expression difference after the application of mechanical force (107 were known lncRNAs, 67 of which showed a downward trend, and 40 of which showed an upward trend. 1 252 were novel lncRNAs, 496 of which showed a downward trend, and 756 of which showed an upward trend). Twelve lncRNAs (6 known, 6 unknown) with large differences in the expression levels and a sum of fpkm greater than 5 were selected for qRT-PCR verification of expression in the two groups of hPDLSCs. The expression trend of most of the chosen lncRNAs are consistent with the high-throughput sequencing results (Fig. 2B). Among them, the decrease of SNHG8 after the mechanical force showed excellent stability. These data indicate the potential relationship between SNHG8 and mechanical force in hPDLSCs.

SNHG8 has a negative effect on osteogenic differentiation of PDLSCs under mechanical force

To determine the effect of SNHG8 on hPDLSCs under stretched, we performed a series of experiments. First, to identify the time point at which there is the most significant change in SNHG8 expression under mechanical force, we evaluated the expression of SNHG8 in hPDLSCs after 6, 12, and 24 hours of stretching. The results showed that SNHG8 had the most significant decline after 6 hours of mechanical force (Fig. 3A). We use the lentivirus for the SNHG8 knockdown. To find out a suitable MOI value, we used sh-SNHG8-1# and sh-SNHG8-2# to conduct a preliminary experiment. Although the MOI of 50 showed the higher transfection efficiency, the cells morphology changed from a long spindle shape to an irregular multi-synaptic shape. We decided that MOI of 30 was the best MOI value and transfection time of 24 hours that have a high transfection efficiency with no effect on cell activity (Fig. 3B). The most efficacious target was sh-SNHG8-2# (Fig. 3C). Fluorescence observation and qRT-PCR verification were used to verify the transfection efficiency. Mechanical force was separately applied to untransfected hPDLSCs (Control group), hPDLSCs transfected with empty plasmids (sh-NC group), and hPDLSCs transfected with effective lentivirus (sh-SNHG8 group). The qRT-PCR and western blot results showed that the expression of ALP was increased in the sh-SNHG8 group after being stretched, and RUNX2 in the sh-SNHG8 group expressed higher after stretching (Fig. 3D-F). These data confirmed that SNHG8 has a negative effect on the expression osteogenic differentiation relative genes of hPDLSCs under mechanical force.

SNHG8 has a negative effect on the osteogenic-induced osteogenic differentiation of PDLSCs

To investigate the function of SNHG8 in the osteogenic induced osteogenic differentiation of PDLSCs, we detected the expression level of SNHG8 after osteogenic induction. Interestingly, with the osteogenic induction of hPDLSCs, except for the fluctuation in the seventh day of induction, the expression level of SNHG8 showed a significant and stable decrease (Fig. 4A). Which may suggest the negative influence of SNHG8 during osteogenic differentiation of PDLSCs. To further confirm the effect of SNHG8 on the osteogenic differentiation of hPDLSCs, we cultured the control group, sh-NC group, and sh-SNHG8 group by mineralization induction medium. The qRT-PCR and western blot results showed significantly higher ALP expression in the sh-SNHG8 group after induction. RUNX2 expression, however, was more significantly upregulated in the non-induced group (Fig. 4B-D). We considered it may be because RUNX2 usually changes in the early stage of osteogenesis, and this kind of change is not so obvious when the induction time endured long. ALP staining (Fig. 4E) and Alizarin Red S staining (Fig. 4F, G) showed that more mineralized nodules were produced in the SNHG8 knockdown groups. These results show that downregulated of SNHG8 can significantly increase osteogenic differentiation in hPDLSCs.

The reduction of SNHG8 has a positive effect on osteogenic differentiation *in vivo*

We then decided to test whether the change of SNHG8 expression after receiving mechanical force *in vivo* had a similar reaction with cells experiments *in vitro*. According to previews studys (38), analogous genes may have similar functions. Therefore, we detected the SNHG8's homologous gene in rats, Smim4, after tooth movement of wistar rats (Fig. 5A, B). The qRT-PCR results showed that the Smim4 level in the periodontal tissue of the mechanical force side decreased steadily from 3 day to 14 days during rats'

tooth movement, and returned to the normal level by 21 days (Fig. 5C). It proved that the expression of the Smim4 gene has decreased during the early stage of tooth movement *in vivo*. To figure out whether the change of SNHG8 expression can also alter the ability of osteogenic differentiation, we implanted control group, sh-NC group, and sh-SNHG8 group PDLSCs under the back of nude mice. The results of Masson's trichrome staining and SafraninO-staining (Fig. 5D) showed that the sh-SNHG8 group formed more collagen fibers in nude mice, which is the necessary matrix for bone formation. In addition, the sh-SNHG8 group also had obvious red stained area of glycoprotein, which suggested cartilage formation. The formation of cartilage also suggests that the sh-SNHG8 group has better bone formation potential.

Expression level of SNHG8 correlates with EZH2

Compering to the 18S probe which located in the cytoplasm and the U6 probe which located in the nucleus, the SNHG8 probe of FISH assay indicated that SNHG8 located in both cytoplasm and nucleus, but most in nucleus (Fig. 6A). The separately detection of SNHG8 from cytoplasm and nucleus also supported these results (Fig. 6B). Since several researches have shown that lncRNAs in the nucleus can regulate physiological or pathological process by interacting with PRC2 (39-41), we considered that SNHG8 may also regulate the osteogenic differentiation of hPDLSCs through this pathway. We detected the RNA and protein levels of the main subunits of the PRC2 complex in the control, sh-NC and sh-SNHG8 groups. The qRT-PCR and western blot results showed that the RNA and protein levels of EZH2 and SUZ12 in the knockdown group were significantly reduced (Fig. 6C-E). In hPDLSCs with EZH2, EED and SUZ12 knockdown (Fig. 6F), the expression level of SNHG8 was also significantly decreased (Fig. 6G). These data suggest that SNHG8 can interact with PRC2, especially EZH2.

SNHG8 regulates osteogenic differentiation under mechanical force through EZH2

To confirm the osteogenic relevance of PRC2, we tested the expression of the three main subunits of PRC2 in cells under mineralized induction at different time points. The RNA expression of EZH2 decreased steadily with the increase of mineralized induction time, and the expression level of SUZ12 decreased during the osteogenic induction period, but fluctuated during the process. However, the expression level of EED did not decrease significantly during the process of osteogenic induction (Fig. 7A). To further confirm whether EZH2, SUZ12, and EED have effects on osteogenic differentiation, we knocked down these three major subunits with small interfering RNA (siRNA) and short hairpin RNA (shRNA), and then performed osteogenic induction of control, negative control and PRC2 knockdown groups. The mRNA expression of ALP and RUNX2 in EZH2-knockdown group was significantly increased, the expression of ALP and RUNX2 in the SUZ12 knockdown group had distinct increase after 7 days of induction, and there is no apparent change of ALP and RUNX2 in the EED knockdown group (Fig. 7B). ALP staining (Fig. 7C) and Alizarin Red S staining (Fig. 7D, E) also showed that more mineralized nodules were produced in the EZH2 and SUZ12 knockdown groups. In general, PRC2 did have a negative effect on the osteogenic differentiation of hPDLSCs, which may be the reason why SNHG8 negatively regulates osteogenic differentiation.

Discussion

Tooth movement based on the remodeling of alveolar bone is the basis of orthodontics. A comprehensive and systematic understanding of cellular changes promotes a better understanding of physiological responses in clinical orthodontics. Although some studies have focused on lncRNAs related to osteogenic differentiation (30), mechanically sensitive lncRNAs and their influence on the osteogenic differentiation of periodontal-derived stem cells are still unclear.

In our research, the lncRNA was chosen for further research due to the significant change after being stretched, SNHG8, has been reported to regulate the progression of non-small-cell lung cancer by sponging miR-542-3p (42). Coincidentally, miR-542-3p was proved to negatively regulates the osteogenic differentiation of vascular muscle smooth cells by targeting bone morphogenetic protein 7 (43). Accordingly, since the interacting between SNHG8 and miR-543-3p has been confirmed, SNHG8 may have the same regulatory ability on negatively regulating osteogenic differentiation. In this paper, our cell experiments in vitro and animal experiments in vivo both provided credible results. Interestingly, according to the results of animal experiments, the SNHG8 knockdown group not only showed greater collagen fibers, but also formed more obvious cartilage compared with the non-transfected group. The effect of SNHG8 on chondrogenic differentiation is not discussed in this paper, but the significantly enhanced ability of chondrogenic differentiation after knockdown SNHG8 may be able to indicate the regulation to differentiation of stem cells by SNHG8.

According to the conclusions of previews studies, we can infer that most lncRNAs present in the nucleus can direct chromatin modifiers to specific genomic sites (17, 22), for example, PRC2 and histone H3 lysine 9 methyltransferase-mediated DNA trimethylation (44). Because SNHG8 is mainly located in the nucleus and lncRNAs may interact with PRC2 to regulate gene expression at the transcription or post-transcription level (45–47), we considered its effect on osteogenic differentiation under mechanical force may be related to epigenetic genes. PRC2 is an epigenetic inhibitor necessary for development in vivo and differentiation of embryonic stem cells in vitro (48), and mainly acts as a transcriptional inhibitor through the trimethylation of H3K27 histones, which is the core feature of achieving chromatin silencing (49). A recent study confirmed the direct interaction between SNHG8 and EZH2 (24), the main subunit of PRC2 and the key regulatory factor in epigenetics. Therefore, we were interested in determining if it has a regulatory in osteogenic differentiation and whether this role contributes to the process and mechanism of alveolar bone reconstruction in tooth movement, which prompted us to conduct a series of studies on the effect of PRC2 on osteogenic differentiation. As an epigenetic regulator, EZH2 is related to MSC osteogenic differentiation, and have been reported to regulate osteogenesis-related genes such as RUNX2. For example, not only osteogenic differentiation can lead to decreased binding of EZH2, SUZ12, and H3K27 trimethylation at the RUNX2 promoter (28), EZH2 can also inhibit RUNX2 expression and subsequent osteoblast differentiation (50). Combined with the fact that EZH2 can interact with SNHG8, and SNHG8 has been confirmed by us to have a negative regulatory effect on the osteogenic differentiation of PDLSCs, we preliminarily inferred and verifieded the hypothesis that EZH2 may also negatively regulate PDLSCs. After confirming the close relationship between SNHG8 and EZH2, we

verified the important role of EZH2 on the osteogenic differentiation of PDLSCs, which is consistent with the conclusion of the above studys, and further suggested the possible relationship between EZH2 and the applying of mechanical force. In our experiments, despite SNHG8 cannot encode a protein, which means it cannot regulate physiological or pathological processes by forming a form of a protein with specific functions. However, after knocking down SNHG8 or EZH2, the expression of the other decreased, which indicated that there is an interaction between these two genes. Their interaction is a solid basis for SNHG8 to perform regulatory effects without directly encoding proteins. We believe that this process not only reveals the regulation of non-coding RNA, but may also reveal the epigenetic regulation of mechanical forces acting on cells and tissues.

Our study prospectively predicted and confirmed the effect of mechanically sensitive lncRNA SNHG8 on the osteogenic differentiation of PDLSCs. We found that SNHG8 has a negative effect on osteogenic differentiation from epigenetics aspect, verified the connection between SNHG8 and EZH2, and confirmed the role of EZH2 and other PRC2 subunits in the osteogenic differentiation of PDLSCs. The undeniable limitation of this study is that no specific changes of downstream of EZH2 (such as the perform of H3K27) have been studied, and it has not verified whether EZH2 can directly respond to mechanical stimulation. However, our study stimulates new ideas for future research into the effect of genes related to cell differentiation under mechanical force and the mechanistic relationship between lncRNAs and epigenetic regulators.

Conclusion

Our results provide a solid evidence for the mechanical force-sensitive lncRNA SNHG8 to regulate the osteogenic differentiation PDLSCs through EZH2. It provides a new idea for non-coding RNA to regulate cell differentiation through coding RNA. In addition, it can act as a theoretical basis for further clinical application of genetic engineering.

Abbreviations

PDLSCs: Periodontal ligament stem cells;

lncRNA: long non-coding RNA;

qRT-PCR: quantitative reverse transcription polymerase chain reaction;

SNHG8: Small nucleolar RNA host gene 8;

EZH2: Enhancer of zeste homolog 2;

PRC2: Polycomb repressive complex 2;

MSC: Mesenchymal stem cell;

ALP: Alkaline phosphatase;

RUNX2: Runt-related transcription factor 2;

EED: Embryonic ectoderm development;

SUZ12: Suppressor of zeste 12;

TBS-T: Tris-buffered saline solution;

FISH: Fluorescence *in situ* hybridization;

FPKM: Fragments Per Kilobase of exon model per Million mapped fragments;

MOI: Multiplicity of Infection

CPC: cetyl pyridinium chloride

Declarations

Ethics approval and consent to participate

All protocols for treating periodontal ligament tissues were performed in accordance with relevant guidelines and regulations. This study was approved by the Research Ethics Committee of Shandong University (No. G201401601). Informed consent was obtained from the donors and their parents before treatment. The research methods of animal experiments in this study are consistent with routine, and the experimental design was confirmed with the principles of animal protection. This study was approved by the Committee on the Ethics of Animal Experiments of Shandong University (No. 20190503).

Consent for publication

Not applicable.

Availability of data and materials

The datasets used and/or analysed during the current study are available from the corresponding author on reasonable request.

Competing interests

The authors have declared that no competing interest exists.

Funding

This study was supported by grants from the National Natural Science Foundation of China (Grant Nos: 81771030 and 82071080) and Construction Engineering Special Fund of Taishan Scholars (Grant No:

tsqn201611068).

Authors' contributions

FW conceived and designed the experiments. ZZ performed the experiments. QH and XZ assisted the experiments *in vitro*. XZ assisted the animal experiments *in vivo*. ZZ, QH, XZ, and XL analyzed the data. ZZ wrote the paper. FW revised the manuscript. All authors have read and approved the manuscript.

Acknowledgements

Special thanks to Songtao Zhang and Aimin Li for the assistance they provided throughout the study.

Authors' information (optional)

[1] Department of orthodontics, School and Hospital of Stomatology, Cheeloo College of Medicine, Shandong University & Shandong Key Laboratory of Oral Tissue Regeneration & Shandong Engineering Laboratory for Dental Materials and Oral Tissue Regeneration.

References

1. Gay IC, Chen S, MacDougall M. Isolation and characterization of multipotent human periodontal ligament stem cells. Orthod Craniofac Res. 2007;10(3):149–60.
2. Seo BM, Miura M, Gronthos S. Investigation of multipotent postnatal stem cells from human periodontal ligament. (vol 364, pg 149, 2004). Lancet. 2004;364(9447):1756-.
3. Sharpe PT. Dental mesenchymal stem cells. Development. 2016;143(13):2273–80.
4. Henneman S, Von den Hoff JW, Maltha JC. Mechanobiology of tooth movement. Eur J Orthodont. 2008;30(3):299–306.
5. Chadipiralla K, Yochim JM, Bahuleyan B, Huang CYC, Garcia-Godoy F, Murray PE, et al. Osteogenic differentiation of stem cells derived from human periodontal ligaments and pulp of human exfoliated deciduous teeth. Cell Tissue Res. 2010;340(2):323–33.
6. Meikle MC. The tissue, cellular, and molecular regulation of orthodontic tooth movement: 100 years after Carl Sandstedt. Eur J Orthodont. 2006;28(3):221–40.
7. Kawarizadeh A, Bourauel C, Gotz W, Jager A. Early responses of periodontal ligament cells to mechanical stimulus in vivo. J Dent Res. 2005;84(10):902–6.
8. Huang HM, Yang RL, Zhou YH. Mechanobiology of Periodontal Ligament Stem Cells in Orthodontic Tooth Movement. Stem Cells Int. 2018;2018.
9. Zhang LQ, Liu WJ, Zhao JD, Ma XJ, Shen L, Zhang YJ, et al. Mechanical stress regulates osteogenic differentiation and RANKL/OPG ratio in periodontal ligament stem cells by the Wnt/beta-catenin pathway. Bba-Gen Subjects. 2016;1860(10):2211–9.
10. Vining KH, Mooney DJ. Mechanical forces direct stem cell behaviour in development and regeneration. Nat Rev Mol Cell Bio. 2017;18(12):728–42.

11. Wei FL, Wang CL, Zhou GY, Liu DX, Zhang XF, Zhao YH, et al. The effect of centrifugal force on the mRNA and protein levels of ATF4 in cultured human periodontal ligament fibroblasts. Arch Oral Biol. 2008;53(1):35–43.
12. Wei FL, Wang JH, Ding G, Yang SY, Li Y, Hu YJ, et al. Mechanical Force-Induced Specific MicroRNA Expression in Human Periodontal Ligament Stem Cells. Cells Tissues Organs. 2014;199(5–6):353–63.
13. Wei FL, Liu DX, Feng C, Zhang F, Yang SY, Hu YJ, et al. microRNA-21 Mediates Stretch-Induced Osteogenic Differentiation in Human Periodontal Ligament Stem Cells. Stem Cells Dev. 2015;24(3):312–9.
14. Wang H, Feng C, Li MY, Zhang ZJ, Liu JN, Wei FL. Analysis of lncRNAs-miRNAs-mRNAs networks in periodontal ligament stem cells under mechanical force. Oral Dis. 2021;27(2):325–37.
15. Iyer MK, Niknafs YS, Malik R, Singhal U, Sahu A, Hosono Y, et al. The landscape of long noncoding RNAs in the human transcriptome. Nat Genet. 2015;47(3):199-+.
16. Reon BJ, Dutta A. Biological Processes Discovered by High-Throughput Sequencing. Am J Pathol. 2016;186(4):722–32.
17. Rinn JL, Chang HY. Genome Regulation by Long Noncoding RNAs. Annu Rev Biochem. 2012;81:145–66.
18. Thomson DW, Dinger ME. Endogenous microRNA sponges: evidence and controversy. Nat Rev Genet. 2016;17(5):272–83.
19. Salmena L, Poliseno L, Tay Y, Kats L, Pandolfi PP. A ceRNA Hypothesis: The Rosetta Stone of a Hidden RNA. Language? Cell. 2011;146(3):353–8.
20. Schmitt AM, Chang HY. Long Noncoding RNAs in Cancer Pathways. Cancer Cell. 2016;29(4):452–63.
21. Yoon JH, Abdelmohsen K, Gorospe M. Functional interactions among microRNAs and long noncoding RNAs. Semin Cell Dev Biol. 2014;34:9–14.
22. Batista PJ, Chang HY. Long Noncoding RNAs: Cellular Address Codes in Development and Disease. Cell. 2013;152(6):1298–307.
23. Flynn RA, Chang HY. Long Noncoding RNAs in Cell-Fate Programming and Reprogramming. Cell Stem Cell. 2014;14(6):752–61.
24. Qu XH, Li YY, Wang L, Yuan NX, Ma M, Chen Y. LncRNA SNHG8 accelerates proliferation and inhibits apoptosis in HPV-induced cervical cancer through recruiting EZH2 to epigenetically silence RECK expression. J Cell Biochem. 2020;121(10):4120–9.
25. Huang LN, Jiang XM, Wang ZD, Zhong XY, Tai S, Cui YF. Small nucleolar RNA host gene 1: A new biomarker and therapeutic target for cancers. Pathol Res Pract. 2018;214(9):1247–52.
26. Cui PL, Zhao XY, Liu JL, Chen XD, Gao Y, Tao K, et al. miR-146a interacting with lncRNA EPB41L4A-AS1 and lncRNA SNHG7 inhibits proliferation of bone marrow-derived mesenchymal stem cells. J Cell Physiol. 2020;235(4):3292–308.

27. Ma QH, Qi XQ, Lin XN, Li L, Chen LB, Hu W. LncRNA SNHG3 promotes cell proliferation and invasion through the miR-384/hepatoma-derived growth factor axis in breast cancer. Hum Cell. 2020;33(1):232–42.
28. Wei YK, Chen YH, Li LY, Lang JY, Yeh SP, Shi B, et al. CDK1-dependent phosphorylation of EZH2 suppresses methylation of H3K27 and promotes osteogenic differentiation of human mesenchymal stem cells. Nat Cell Biol. 2011;13(1):87–211.
29. Schwarz D, Varum S, Zemke M, Scholer A, Baggiolini A, Draganova K, et al. Ezh2 is required for neural crest-derived cartilage and bone formation. Development. 2014;141(4):867–77.
30. Deng LD, Hong H, Zhang XQ, Chen DR, Chen ZY, Ling JQ, et al. Down-regulated lncRNA MEG3 promotes osteogenic differentiation of human dental follicle stem cells by epigenetically regulating Wnt pathway. Biochem Bioph Res Co. 2018;503(3):2061–7.
31. Wei FL, Qu CY, Song TL, Ding G, Fan ZP, Liu DY, et al. Vitamin C treatment promotes mesenchymal stem cell sheet formation and tissue regeneration by elevating telomerase activity. J Cell Physiol. 2012;227(9):3216–24.
32. Wei FL, Song TL, Ding G, Xu JJ, Liu Y, Liu DY, et al. Functional Tooth Restoration by Allogeneic Mesenchymal Stem Cell-Based Bio-Root Regeneration in Swine. Stem Cells Dev. 2013;22(12):1752–62.
33. Gu XG, Li MY, Jin Y, Liu DX, Wei FL. Identification and integrated analysis of differentially expressed lncRNAs and circRNAs reveal the potential ceRNA networks during PDLSC osteogenic differentiation. Bmc Genet. 2017;18.
34. Borodina T, Adjaye J, Sultan M. A Strand-Specific Library Preparation Protocol for Rna Sequencing. Method Enzymol. 2011;500:79–98.
35. Collinson A, Collier AJ, Morgan NP, Sienerth AR, Chandra T, Andrews S, et al. Deletion of the Polycomb-Group Protein EZH2 Leads to Compromised Self-Renewal and Differentiation Defects in Human Embryonic Stem Cells. Cell Rep. 2016;17(10):2700–14.
36. Lin X, Yu YN, Zhao HP, Zhang YY, Manela J, Tonetti DA. Overexpression of PKC alpha is required to impart estradiol inhibition and tamoxifen-resistance in a T47D human breast cancer tumor model. Carcinogenesis. 2006;27(8):1538–46.
37. Zielske SP, Stevenson M. Importin 7 may be dispensable for human immunodeficiency virus type 1 and simian immunodeficiency virus infection of primary macrophages. J Virol. 2005;79(17):11541–6.
38. Durand PM, Hazelhurst S, Coetzer TL. Evolutionary rates at codon sites may be used to align sequences and infer protein domain function. Bmc Bioinformatics. 2010;11.
39. Yang MH, Zhao L, Wang L, Wen OY, Hu SS, Li WL, et al. Nuclear lncRNA HOXD-AS1 suppresses colorectal carcinoma growth and metastasis via inhibiting HOXD3-induced integrin 3 transcriptional activating and MAPK/AKT signalling. Mol Cancer. 2019;18.
40. Wutz A. Gene silencing in X-chromosome inactivation: advances in understanding facultative heterochromatin formation. Nat Rev Genet. 2011;12(8):542–53.

41. Zhao J, Sun BK, Erwin JA, Song JJ, Lee JT. Polycomb Proteins Targeted by a Short Repeat RNA to the Mouse X Chromosome. Science. 2008;322(5902):750–6.
42. Chen C, Zhang Z, Li J, Sun Y. SNHG8 is identified as a key regulator in non-small-cell lung cancer progression sponging to miR-542-3p by targeting CCND1/CDK6 (vol 11, pg 6081, 2018). Oncotargets Ther. 2018;11:8013-.
43. Liu H, Wang HW, Yang SJ, Qian DH. Downregulation of miR-542-3p promotes osteogenic transition of vascular smooth muscle cells in the aging rat by targeting BMP7. Hum Genomics. 2019;13(1).
44. Margueron R, Reinberg D. The Polycomb complex PRC2 and its mark in life. Nature. 2011;469(7330):343–9.
45. Blanco MR, Guttman M. Re-evaluating the foundations of lncRNA-Polycomb function. Embo J. 2017;36(8):964–6.
46. McHugh CA, Chen CK, Chow A, Surka CF, Tran C, McDonel P, et al. The Xist lncRNA interacts directly with SHARP to silence transcription through HDAC3. Nature. 2015;521(7551):232-+.
47. Sun M, Nie FQ, Wang YF, Zhang ZH, Hou JK, He DD, et al. LncRNA HOXA11-AS Promotes Proliferation and Invasion of Gastric Cancer by Scaffolding the Chromatin Modification Factors PRC2, LSD1, and DNMT1. Cancer Res. 2016;76(21):6299–310.
48. Kaneko S, Son J, Shen SS, Reinberg D, Bonasio R. PRC2 binds active promoters and contacts nascent RNAs in embryonic stem cells. Nat Struct Mol Biol. 2013;20(11):1258-U275.
49. Simon JA, Kingston RE. Mechanisms of Polycomb gene silencing: knowns and unknowns. Nat Rev Mol Cell Bio. 2009;10(10):697–708.
50. Zhu L, Xu PC. Downregulated LncRNA-ANCR promotes osteoblast differentiation by targeting EZH2 and regulating Runx2 expression. Biochem Bioph Res Co. 2013;432(4):612–7.

Tables

Table 1. The primers of lncRNAs and mRNAs

ID	Primer(5' to 3')	Primer Sequence
TCONS_00194658 (Human)	forward	ACTTGCCTCTTCTGATTGCCT
	reverse	GTCTCCAACACTCTGCAAGG
TCONS_00023760 (Human)	forward	AAAGAATGCCTGGAGGGCTG
	reverse	AACATGCTGCTTTTAATCCATGT
TCONS_00142327 (Human)	forward	TTCAGTGTTAGTCATATACCAGTGT
	reverse	TGCAGACCCTTCCTCCACA
TCONS_00124579 (Human)	forward	GACAGGTCTGGAGCACACTC
	reverse	GGAGCTAAACCCAGTGGACC
TCONS_00173743 (Human)	forward	TCTTGTGATCCGAGCCACTTC
	reverse	AACTCCAGCCCTATCAGGTG
TCONS_00242019 (Human)	forward	AGAGCACGTCATACTTCCAGG
	reverse	TTAGCTTCCTTGCGGAAATGC
OSER1-AS1 (Human)	forward	TGAGGTGTATGCAGTGGAGC
	reverse	TCACACTAGGCAGGAAGGGA
RP11-1002K11 (Human)	forward	GGGATTTGTGGATCACTTGCCTT
	reverse	AAAGAGCAGGGCTTGACATCTGA
MIR22HG (Human)	forward	CGGGACTGAATGGGGGTTAAT
	reverse	ACGCACGAGCTTAGGGTAGA
LINC00968 (Human)	forward	ATGAGGGACCTGCTGGAAGA
	reverse	GAGACATGAGGTGCCAGGAG
SNHG9 (Human)	forward	CTGAGTGCTCTTGCCCG
	reverse	TGGGAGGACCAGTGTCCTAAG
SNHG8 (Human)	forward	ATTAGGTGAAAGTCGCCGGG
	reverse	TCAAACTGACGGTTCTCGGG
ALP (Human)	forward	CCACGTCTTCACATTTGGTG
	reverse	AGACTGCGCCTGGTAGTTGT
RUNX2 (Human)	forward	CGAATTGGCAGCACGCTATTAA
	reverse	GTCGCCAAACAGATTCATCCA

EZH2 (Human)	forward	GTACACGGGGATAGAGAATGTGG
	reverse	GGTGGGCGGCTTTCTTTATCA
EED (Human)	forward	AAAGATGCTTGCATTGGGCA
	reverse	TGTCGAATAGCAGCACCACA
SUZ12 (Human)	forward	ACATCAAAAGCTTGTCAGCTC
	reverse	GGCACCTGCTTTTTACCTGTG
GAPDH (Rat)	forward	TCATGGGTGTGAACCATGAGAA
	reverse	GGCATGGACTGTGGTCATGAG
Smin4 (Rat)	forward	GCCAGGAGACCTTCTATGATGT
	reverse	ATCTTCCAGCCTTCTCTGATACTG
gapdh (Rat)	forward	TCTCTGCTCCTCCCTGTTCT
	reverse	ATCCGTTCACACCGACCTTC

Figures

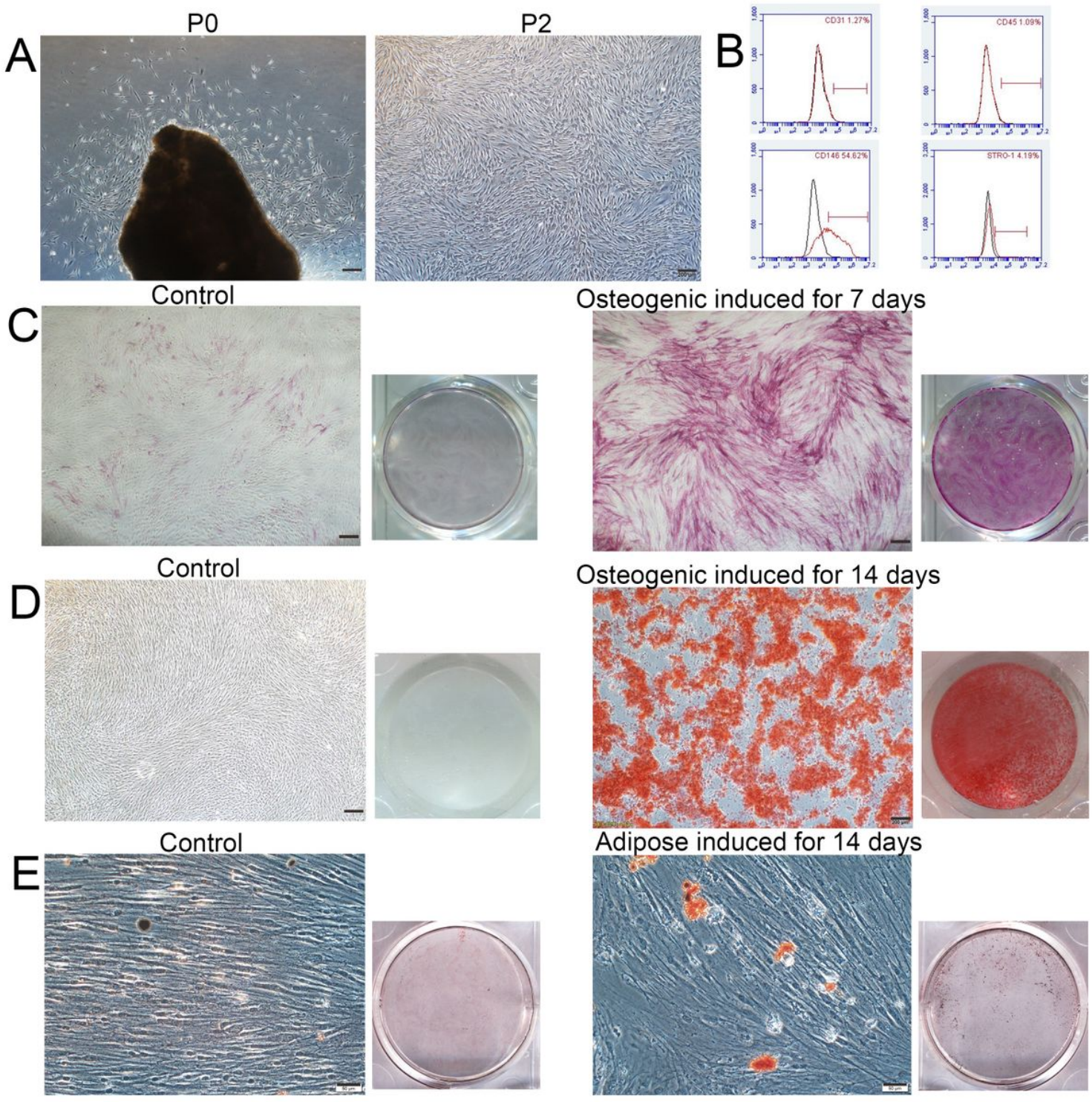

Figure 1

Cell culture and biological characteristics identify A. Cell morphology of periodontal ligament stem cells (Scale bar=200μm). B. The expression of CD31, CD45, CD146 and Stro-1 tested by flow cytometry. C, D. The ALP staining and Alizarin Red staining results of control group and osteogenic induced for 7 or 14 days group (Scale bar=200μm). E. The Oil Red O staining results of control group and adipose induced for 14 days group (Scale bar=200μm).

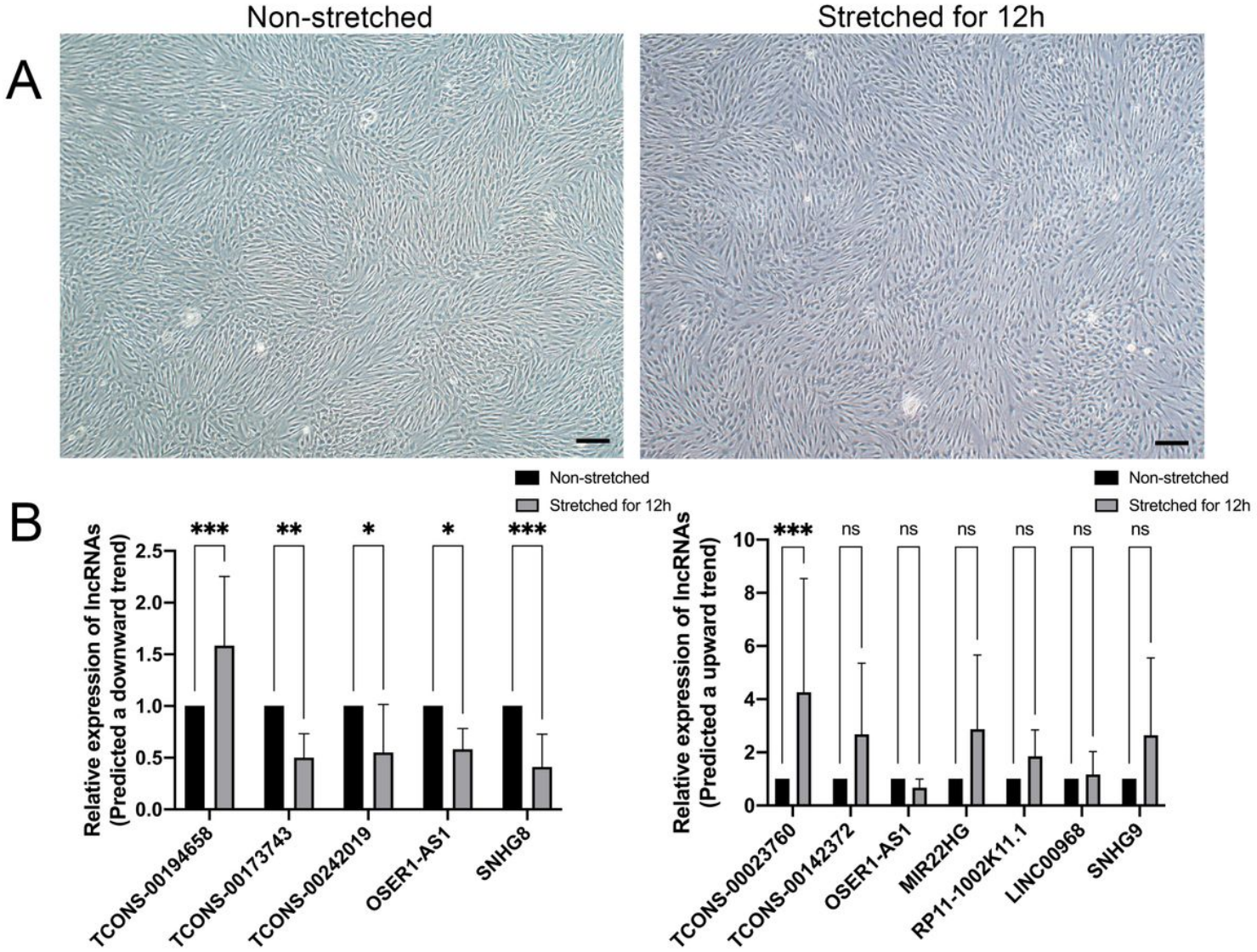

Figure 2

Identification of mechanical force-sensitive lncRNA A. Cell morphology of the non-stretched and stretched for 12 hours group (Scale bar=200μm). B. The verification of selected lncRNAs expression between non-stretched and stretched for 12 hours group (Tested by qRT-PCR. *P<0.05. **P<0.01. ***P<0.001).

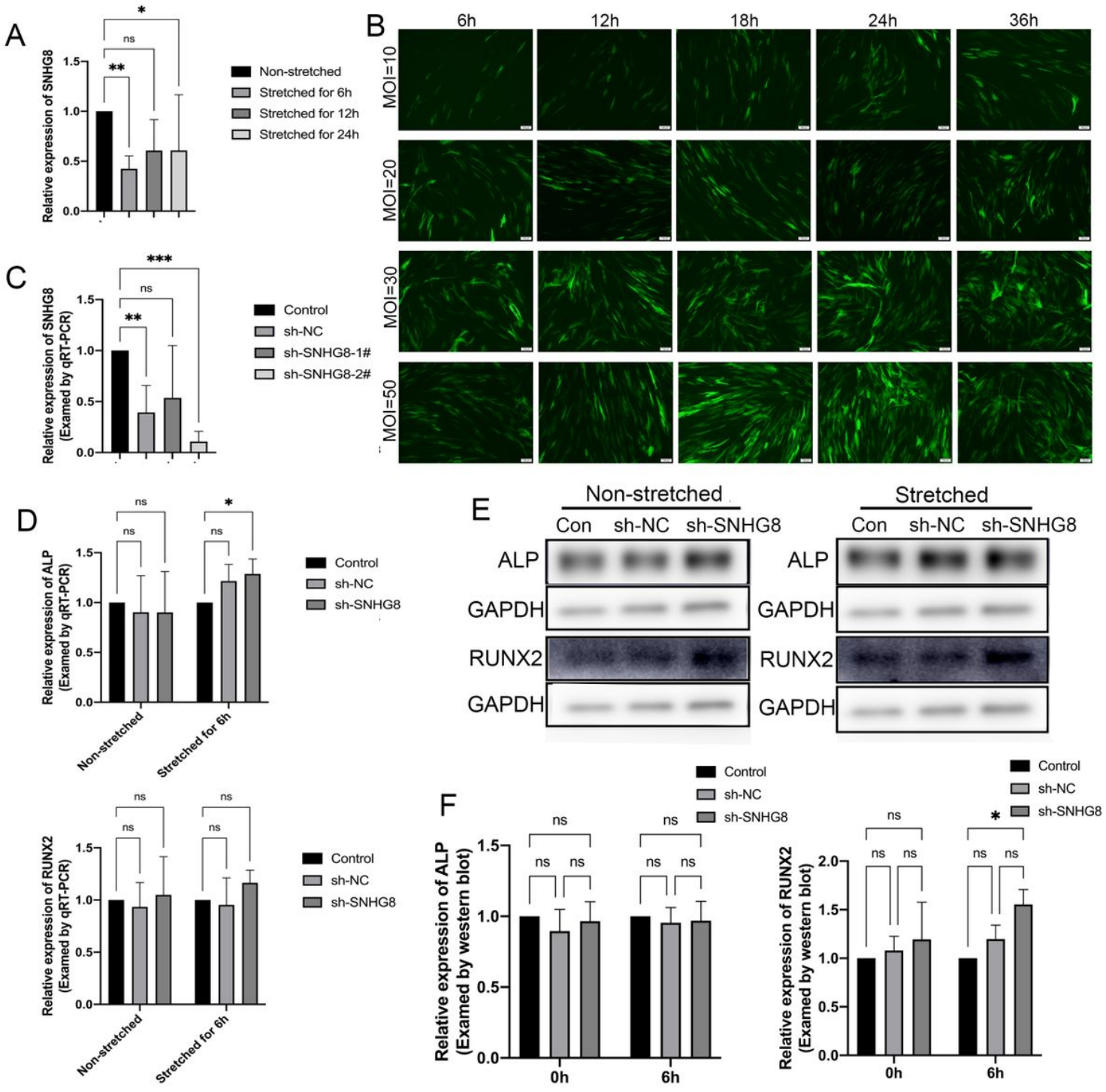

Figure 3

SNHG8 has a negative effect on osteogenic differentiation of PDLSCs under mechanical force A. The relative expression of SNHG8 in PDLSCs after being stretched for different time (*P<0.05. **P<0.01). B. Lentivirus transfection status under different MOI and different transfect time (Scale bar=200μm). C. The relative expression of SNHG8 after transfection (Tested by qRT-PCR. **P<0.01. ***P<0.001). D. The relative expression of ALP and RUNX2 before and after being stretched in control group, sh-NC group and sh-SNHG8 group (Tested by qRT-PCR. *P<0.05). E. The relative expression of ALP and RUNX2 before and

after being stretched in control group, sh-NC group and sh-SNHG8 group (Tested by western blot). F. Quantification of western blot results (*P<0.05).

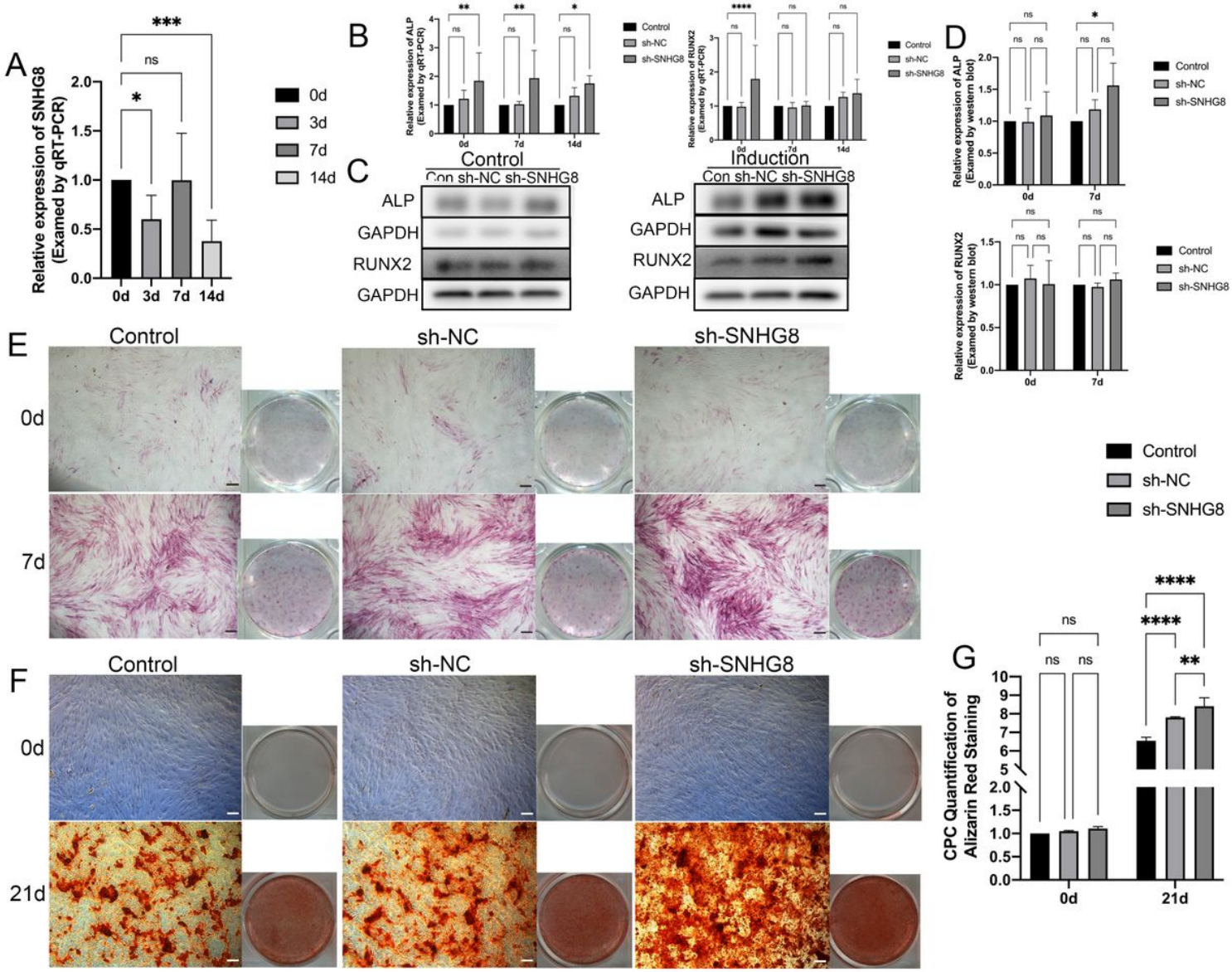

Figure 4

SNHG8 has a negative effect on the osteogenic differentiation of PDLSCs while being osteogenic induced A. The relative expression of SNHG8 in PDLSCs after osteogenic induction for different time (Tested by qRT-PCR. *P<0.05. ***P<0.001). B. The relative expression of ALP and RUNX2 after osteogenic induction in control group, sh-NC group and sh-SNHG8 group (Tested by qRT-PCR. *P<0.05. **P<0.01. ****P<0.0001). C. The relative expression of ALP and RUNX2 after osteogenic induction in control group, sh-NC group and sh-SNHG8 group (Tested by western blot). D. Quantification of western blot results (*P<0.05). E. The ALP staining results of control group, sh-NC group and sh-SNHG8 group after being osteogenic induced (Scale bar=200μm). F The Alizarin Red staining results of control group, sh-NC group and sh-SNHG8 group after being osteogenic induced (Scale bar=200μm). G. The relative CPC quantification of Alizarin Red staining.

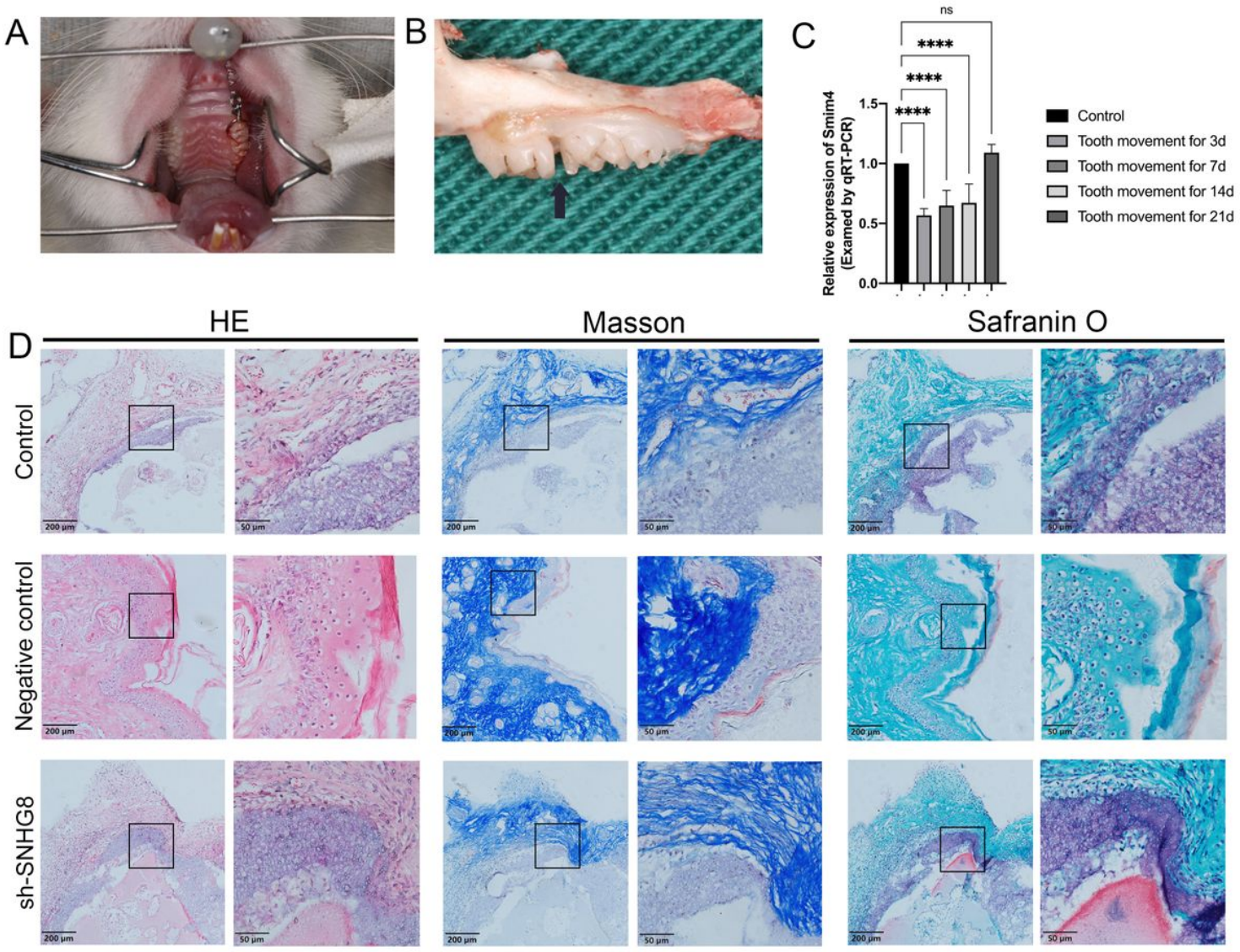

Figure 5

The reduction of SNHG8 has a positive effect on osteogenic differentiation in vivo A. The tooth movement model built in wistar rats. B. The teeth and alveolar bone sample after tooth moving. The arrow shows the interdental space after tooth moving. C. The relative expression level of the homologous gene of SNHG8, Smim4, in PDLSCs and alveolar bone of rats after building tooth moving model for different time (Tested by qRT-PCR. ****P<0.0001). D. The HE staining, Masson's trichrome staining and SafraninO-staining results of control group, sh-NC group, and sh-SNHG8 group PDLSCs' mass formed under the skin of the back of nude mice (Scale bar=200μm/50μm).

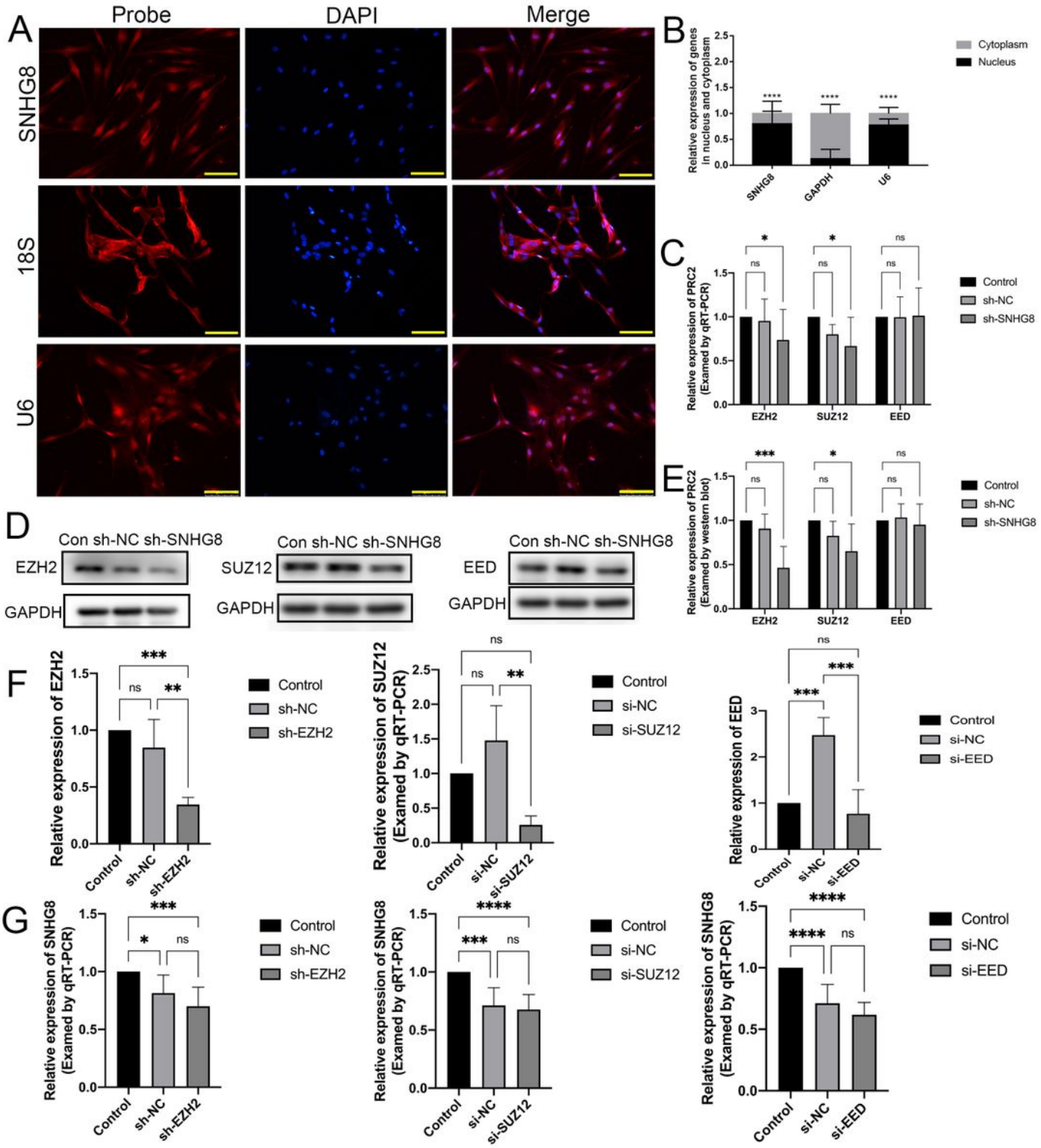

Figure 6

The expression level of SNHG8 correlates with the PRC2 complex A. The sub-cellular localization of SNHG8, 18S, and U6 examined by FISH assay (Scale bar=50μm). B. The relative expression of SNHG8 in the nucleus and cytoplasm (Tested by qRT-PCR. ****P<0.0001). C. The relative expression of EZH2, SUZ12, and EED in control group, sh-NC group and sh-SNHG8 group (Tested by qRT-PCR. *P<0.05). D. The relative expression of EZH2, SUZ12, and EED in control group, sh-NC group and sh-SNHG8 group (Tested

by western blot). E. Quantification of western blot results (*P<0.05. ***P<0.001). F. The relative expression level of EZH2, SUZ12, and SUZ12 after transfection by lentivirus or siRNA (**P<0.01. ***P<0.001). G. The expression of SNHG8 in control group, sh-NC group and PRC2 subunit knockdown group (Tested by qRT-PCR. *P<0.05. ***P<0.001. ****P<0.0001).

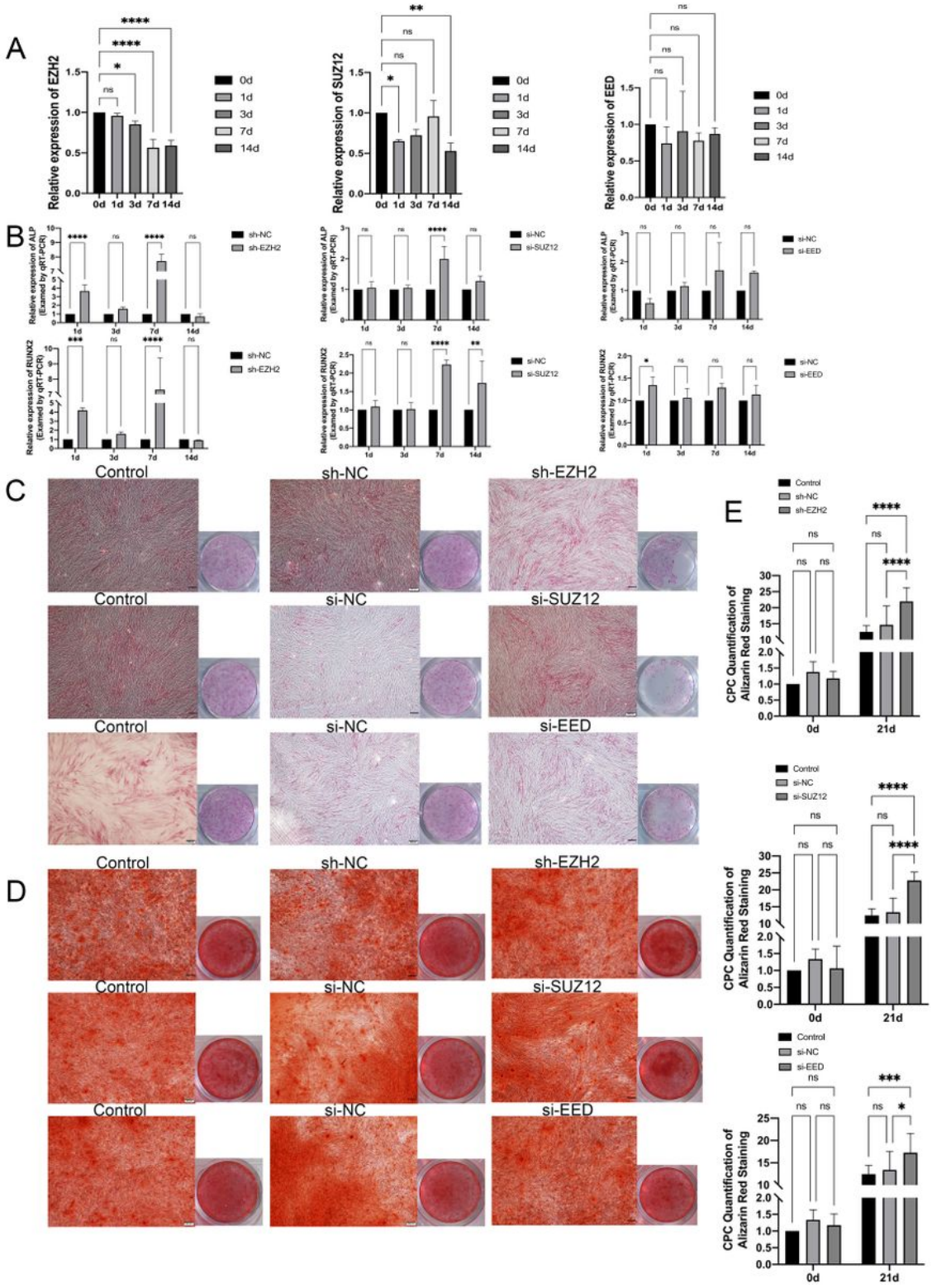

Figure 7

SNHG8 regulates osteogenic differentiation under the action of mechanical force through the PRC2 complex A. The relative expression level of EZH2, SUZ12, and EED in PDLSCs after osteogenic induction for different time (Tested by qRT-PCR. *P<0.05. **P<0.01. ****P<0.0001). B. The expression of ALP and RUNX2 after osteogenic induction in control group and PRC2 knockdown group (Tested by qRT-PCR. ****P<0.0001). C. The ALP staining results of control group, sh-NC group, sh-EZH2 group, si-NC group, si-EED group, and si-SUZ12 group group after osteogenic induction (Scale bar=200μm). D. The Alizarin Red staining results of negative control group, positive control group, sh-NC group, sh-EZH2 group, si-NC group, si-EED group, and si-SUZ12 group group after being osteogenic induced (Scale bar=200μm). E. The relative CPC quantification of Alizarin Red staining.

Supplementary Files

This is a list of supplementary files associated with this preprint. Click to download.

- Supportinginformation.rar